LA-UR-06-0615

Comparison of near infrared and thermal infrared cloud phase detections

Petr Chylek[1], S. Robinson[2], M. K. Dubey[3], M. D. King[4], Q. Fu[2], W. B. Clodius[1]

March 20, 2006

[1]Space and Remote Sensing Sciences, Los Alamos National Laboratory, Los Alamos, New Mexico

[2]Department of Atmospheric Sciences, University of Washington, Seattle, Washington

[3]Earth and Environmental Sciences, Los Alamos National Laboratory, Los Alamos, New Mexico

[4]NASA Goddard Space Flight Center, Greenbelt, Maryland

ABSTRACT

We compare the results of the cloud thermodynamic phase detection that uses (a) the ratio of the near infrared and visible bands, and (b) the brightness temperature difference (BTD) of two thermal infrared bands. We find that the brightness temperature difference algorithm using the MODIS (Moderate Resolution Imaging Spectroradiometer) bands is generally consistent with the expectations based on the retrieval of the cloud top radiative temperature. On the other hand the band ratio (BR) method, which uses near infrared and visible bands, assigns considerably more ice phase compared to the brightness temperature difference method and leads to discrepancies with the expectations based on the cloud top radiative temperature. When the cloud phase algorithm, developed originally for the Department of Energy (DOE) Multispectral Thermal Imager (MTI) research satellite, is applied to the MODIS imagery, the cloud phase assignments are close to the brightness temperature difference results and in better agreement with the expectations based on the cloud top radiative temperature.

1. Introduction

Knowledge of the cloud radiative properties is essential for the understanding and modeling of climate. Cloud thermodynamic phase, the classification of cloud particles as consisting of water, ice or a mixture of the two, greatly affects these properties. The daily study of global cloud extent, phase and other cloud properties as well as aerosol-cloud interactions [*Chylek et al.,* 2006] is essential for climate study. Currently, this is only possible with data from satellite-based instruments.

One of the most versatile satellite instruments for atmospheric remote sensing is the Moderate Resolution Imaging Spectroradiometer (MODIS) [*Kaufman et al.,* 1997; *Tanré et al.,* 1997; *Platnick et al.,* 2003; *King et al.,* 2003] on the Terra and Aqua satellites. MODIS has 36 spectral bands from the visible to the thermal infrared region. The pixel sizes vary from 250m in visible bands to 1km in the infrared spectral region. The MODIS cloud phase product (MOD06 for Terra and MYD06 for Aqua) is a combination of two different cloud phase detection methods, one using near infrared and visible bands ratio and the other the brightness temperature difference of two thermal infrared bands. These band ratio (BR) and brightness temperature difference (BTD) procedures distinguish between liquid water and ice based on the differences in their bulk optical properties specified by refractive indices. The final MODIS cloud phase product combines the MODIS cloud mask, the results of the BTD and the BR detection. It also undergoes a "sanity" check in the form of a comparison of the deduced cloud phase with the retrieved cloud top temperature in which all cloud tops with temperature over 273 K are classified as water and those with cloud top temperature below 238 K as ice. Details of the MODIS cloud phase detection are described in *King et al.* [2004] and the thresholds for separating

water from ice used in the current MOD06 or MYD06 products (*Collection 004*) are listed in *King et al.* [2002].

In the following, we compare the results of cloud thermodynamic phase detection of optically thick clouds using only the band ratio (BR) or only the brightness temperature difference (BTD) parts of the MODIS cloud phase detection algorithm. Such a comparison can demonstrate the strengths or weaknesses of each method, which may be useful for future improvements in cloud phase detection. In addition, with the future deployment of hyper-spectral satellite instrumentation, we will have instruments that will cover the near infrared (NIR) spectral region only and other instruments that will only cover the thermal infrared (TIR). These instruments will need to deduce the cloud thermodynamic phase using only the NIR or only the TIR radiances.

2. Physical Basis: Near Infrared and Visible Bands Ratio (BR) Method

The satellite instrument measures the radiances emitted or reflected by the surface, atmosphere or clouds into the instrument's line of sight. A cloud mask is used when we need to limit the imagery to cloudy parts only. In the case of optically thick clouds the radiances observed by a satellite instrument originate predominantly at or near the cloud top or in the atmospheric layer between the cloud and the satellite.

Radiances reflected by the top cloud layer depend on cloud thickness, cloud particle number density, size, shape [*Mishchenko et al.,*1996; *Fu et al.,*1998; *Yang et al.,* 2005] and phase. If we want to deduce the information concerning the particle phase (water, ice or mixed), we have to (a) select a spectral region where water and ice have distinctly different optical properties, (b) make an effort to minimize the influence of cloud microphysics (particle concentration, size and shape) on the reflected radiances, and (c) stay

away from absorption bands of water vapor and other atmospheric gases. The effect of cloud microphysics on satellite-received radiances cannot be completely eliminated. However, by considering a ratio of radiances instead of radiances themselves and by choosing suitable wavelength regions, the effect can be minimized.

If ice and water particles were of the same shape, size and particle density, the differences between reflected solar radiances from water or ice clouds would depend only on the differences in the refractive indices of water and ice. While the real parts of the refractive indices of water and ice are very similar to each other in the visible and near infrared (VNIR) regions, the imaginary parts are considerably different in particular spectral intervals. The imaginary parts of refractive indices, in addition to dominating absorption, significantly affect particle scattering and, therefore, radiances reflected by clouds.

Fig. 1 shows the imaginary parts of refractive indices of water and ice for the wavelength region from 1.2 to 2.4 μm [*Kou et al.,* 1993; *Gosse et al.,* 1995]. Intermolecular forces modify water vapor absorption bands and transform them into the absorption bands of liquid-phase water and solid-phase ice. Because the absorption peaks of the two phases occur at different wavelengths (due to the differences between average intermolecular forces in water and ice), there are several spectral regions within the NIR where the imaginary parts of the refractive indices of water and ice are significantly different (Fig. 1). Considering the MODIS NIR spectral bands (Table 1), the regions with different imaginary parts of refractive indices are bands 6 (1.63 to 1.65 μm) and 7 (2.10 to 2.16 μm). In both of these regions, the imaginary part of the refractive index of ice is considerably larger (by a factor of about three in MODIS band 6 and by a factor of about two in band 7) than that of water. Consequently, ice particles will absorb more energy

and reflect less compared to water droplets. Therefore, either MODIS band (6 or 7) can be used to distinguish between water and ice cloud particles.

To eliminate the dependence of satellite radiances reflected by clouds on particle concentration, we use the ratio of radiances of two suitably chosen bands instead of an absolute value of radiance in a band of interest. In the VNIR part of the solar spectrum, the imaginary parts of the refractive indices of water and ice are so small that they can be effectively neglected and real parts are essentially the same for both water and ice (about 1.30 ± 0.03). In this region the scattering properties of water and ice are largely independent of material. In order to eliminate the dependence of the detected signal on cloud particle concentration, we can choose any of the MODIS bands within the visible or very near infrared region as long as we stay away from the water vapor absorption bands. For optimal signal-to-noise performance, the MODIS bands 1 and 2 (Table 1) are the best candidates. There are, of course, other MODIS-specific considerations to take into account such as the noise of individual bands and the fact that band 6 works on some, but not all, pixels of the MODIS Aqua instrument. Considering all the factors involved, the NIR part of the current MOD06 (MYD06 for Aqua) cloud phase product [*King et al.,* 2002, 2004] uses the ratio of reflectance of MODIS bands 6 or 7 to a reflectance of the visible band 1 (Table 1). Because band 6 does not work reliably on the MODIS Aqua instrument, we will use MODIS spectral bands 7 and 1 for the band ratio (BR) cloud phase detection.

An alternate possibility for cloud phase detection using the ratio of the NIR spectral bands similar to MODIS 6 and 2 was developed [*Chylek and Borel,* 2004] originally for the DOE Multispectral Thermal Imager (MTI) [*Szymanski and Weber,* 2005]. This

method (denoted as MTI) will be applied later in this report to the MODIS imagery as well.

3. Physical Basis: Brightness Temperature Difference (BTD) Method

In the TIR spectral region, satellite instrument sensors measure the radiances emitted by the cloud top layer (for the case of optically thick clouds) plus the intervening atmosphere. The goal is to find a suitable spectral region in which the emissivity of water will be significantly different from that of ice. At the same time we have stay away from the absorption bands of water vapor and other atmospheric gases. The emissivity of any material is related to its absorbance that in turn is related to the imaginary part of the refractive index [*Hale and Querry,* 1973; *Warren,* 1984; *Gosse et al.,* 1995]. Within the longwave infrared atmospheric window (from about 8 to 13 μm), there is a region between 11 and 12 μm (Fig. 2) where the imaginary parts of the refractive indices of water and ice are distinctly different and there is a region between 8.5 and 10 μm where they are approximately equal to each other.

Considering the MODIS TIR bands (Table 1) and avoiding the region of strong ozone absorption around 9.5μm, we are lead to consider the MODIS bands 31 and 32 (centered approximately around 11 and 12μm, respectively) for bands with different water and ice emissivities and MODIS band 29 (centered around 8.55μm) for the band where emissivities of water and ice are almost the same [*Strabala et al.,* 1994]. To minimize the effect of cloud particle size, we select the bands that are spectrally as close to each other as possible, namely MODIS bands 31 and 29. We could again consider the ratio of band radiances, but instead we transform the radiances into brightness temperatures and calculate their difference.

4. MTI Near Infrared Cloud Phase Detection

The Department of Energy Multispectral Thermal Imager (MTI) has 15 spectral bands with pixel sizes of 5 m in the visible bands and 20 m in the infrared region [*Chylek et al.,* 2003]. The NIR cloud phase detection method [*Chylek and Borel,* 2004] for the MTI was developed independently of the MODIS algorithm. The main difference between the MTI and the MODIS band ratio cloud phase detection is that the MTI detection uses spectral bands that are similar to MODIS bands 6 and 2 instead of the bands 7 and 1 used by the MODIS algorithm (MODIS Terra also uses band 6). The selection of bands for the MTI retrieval was motivated by the earlier stated requirements including the minimization of the particle size effect through the selection of spectral bands that are closer together. Band 6 reflectance is less sensitive to particle size than is band 7 reflectance. When changing the cloud droplet radius from 4 to 20 μm in clouds with optical thickness greater than 5, the MODIS band 6 reflectance changes by about 30% while reflectance within MODIS band 7 changes by over 60% [*King et al.,* 1997].

The method originally developed for the MTI retrieval of mixed phase clouds in the Arctic region [*Chylek and Borel,* 2004] is currently applied here without any adjustment of the threshold values for ice and water phase. Future studies may eventually require some threshold adjustment for different environments as has been done in the case of the MODIS band ration phase detection [*King et al.,* 2002; 2004].

5. Data

For comparison of cloud phase detection algorithms, we have selected five different cloud structures within two MODIS images (Fig. 3). One shows decaying hurricane Katrina on August 30, 2005 and the other shows a group of storms over the Indian Ocean on

December 16, 2004. The images were selected so that most of the cloud groups investigated contained all three types of clouds: water, ice and mixed phase. In our investigation, we use MODIS calibrated radiances at 1 km spatial resolution.

We note that the MODIS VNIR band ratio detection, originally published in connection with the cloud phase determination of Arctic stratus clouds over snow or ice surfaces, has different thresholds designed to distinguish between water and ice clouds in different environments. The thresholds used in our study and described in the following section (Section 6) are MODIS NIR *Collection 4* thresholds [*King et al.,* 2002; 2004] listed in Table 2. The thresholds used for the MODIS TIR retrieval of cloud phase, based on *Baum et al.* [2000], and the threshold for the MTI NIR algorithm [*Chylek and Borel,* 2004] are also given in Table 2. A modified MODIS algorithm, *Collection 005,* that is currently being used by NASA GSFC to re-process MODIS imagery for future use, is described in Section 7.

6. The Results

The results of our analysis are presented in Figs. 4 and 5. The red color indicates regions where ice is expected, while water is designated by green. Yellow regions are mixed phase clouds or clouds with an undetermined cloud phase. The color scheme is defined in detail in Table 3.

We start our discussion of the retrieval results with the August 30, 2005 image containing the Katrina cloud (region I in Fig. 3). To concentrate our investigation on areas covered by optically thick clouds, we apply first the "primitive" cloud mask requiring that the reflectivity in each of the MODIS bands 1, 3 and 4 (for band specification see Table 1) is larger than 0.5. An example of cloud mask performance can be seen in Fig.

4a.

The band ratio (BR) cloud phase detection method suggests ice (red color) over most of the cloudy region and some areas with mixed or an undetermined water/ice composition (yellow color), as shown in Fig. 4b. The brightness temperature difference (BTD) phase detection scheme presents a significantly different water/ice structure (Fig. 4c). The southern part of the Katrina cloud (south on the image is approximately in the downward direction) seems to be predominantly water cloud (green color) that is separated from ice cloud (red) by regions of mixed or undetermined cloud phase. Obviously, the BR and BTD retrieval schemes do not present a consistent picture. Some cloud regions identified as ice in the BR retrieval (Fig. 4b) are classified as water clouds in the BTD retrieval (Fig. 4c).

We use the MODIS band 31 brightness temperature as a proxy to decide which of the two cloud phase structures (water or ice) is more probable to occur. Due to the high emissivity of both water and ice in band 31 (centered around the wavelength of 11 μm), and the typically excellent atmospheric transmission between the cloud top and the satellite, the cloud top brightness temperature for an optically thick cloud is usually no more than 1 K from the physical temperature. Because supercooled water has not been observed at temperatures below 238 K, it seems reasonable to assume that the region of the cloud with cloud top brightness temperatures $T_{11} < 238$ K will consist of ice crystals and that the region with $T_{11} > 275$ K will be composed of water droplets. The region in between 238 K and 275 K can be composed of ice, water or a mixture of water and ice. Band 31 cloud top brightness temperature, T_{11}, is shown in Fig. 4d. In the red regions ($T_{11} <238$ K), we expect ice and in green ones ($T_{11} > 275$ K) water. In yellow regions, we

are ready to accept either ice or water or a mixed phase cloud exists. It is apparent that the BTD cloud phase detection (Fig. 4c) is consistent with the expectation based on the cloud top brightness temperature, while the BR detection (Fig. 4b) is not.

An additional support for the BTD cloud phase detection comes from the MODIS-retrieved cloud particle effective size (Fig. 4f). Small effective radii ($r_{eff} < 15$ μm, green color in Fig. 4f) are typical of water droplets and large radii ($r_{eff} > 30$ μm, red color in Fig. 4f) characterize ice crystals [*Fu,* 1996].

The MTI cloud phase code, when applied to the MODIS images, leads to results shown in Fig. 4e. The MTI cloud phase identification is very similar to the BTD cloud phase detection (Fig. 4c) and agrees with expectations based on the cloud top brightness temperature (Fig. 4d) and cloud particle effective size (Fig. 4f).

The results of the BR, BTD and the MTI cloud phase codes applied to a group of clouds in regions II of Fig. 3 leads to the same conclusion (see Fig. 5). Similar results (not shown) are obtained for the three groups of clouds over the Indian Ocean (regions III to V in Fig. 3). In general, the BR cloud phase detection indicates much more ice than the BTD or the MTI detection and than is suggested by the cloud top radiative temperature.

All of the BR retrievals presented were obtained using the threshold values designated for clouds over the ocean and land (Table 2). If we use the thresholds for clouds over ice and snow [*King et al.,* 2002; 2004], the cloud phase algorithm fails to properly identify the ice. Perhaps some threshold adjustment to values in between those used for clouds over the land and sea and over snow and ice could improve the BR cloud phase detection.

It is essential to establish that the methods that use the NIR and the TIR bands observe the same vertical cloud level. Could it be possible that the TIR penetrates deeper into the cloud responding the liquid water part that is below the top glaciated layer?

Most of the radiation received by the satellite is scattered or emitted by the top layer of the cloud that is within an optical thickness of $\tau < 2$. The optical thickness, τ, is given by

$$\tau = k_{ext} N z \tag{1}$$

where the extinction coefficient $k_{ext} = \pi r^2 Q_{ext}$, with Q_{ext} being the extinction efficiency. N is the number of cloud particles (water droplets or ice crystals) per unit volume, and z is a geometrical thickness of a cloud layer. Setting $\tau = 2$ as an approximate level from which the radiation still can reach the satellite instrument, we have the layer thickness as

$$z = \frac{2}{\pi r^2 Q_{ext} N} \tag{2}$$

Considering for simplicity spherical particles, Q_{ext} can be calculated using the Mie scattering formalism. For typical ice crystal radii ($r > 15$ μm) the extinction efficiencies (at the wavelengths of $\lambda = 2.13$ μm and 11.03 μm) are close to 2 leading to an essentially identical depth of the cloud layer (Eq. 2) sampled by the NIR and TIR bands. More details concerning the depth of cloud penetrated by radiation can be found in *Nakajima and King* [1990] and *Platnick* [2000].

Note that for the comparison of the cloud phase retrievals, we have purposefully chosen difficult cases by selecting groups of clouds that could contain water droplets, ice crystals or a mixture of water droplets and ice crystals. It was within these cases that major differences between individual codes were observed. In the more common simple

cases, where only one phase is present (such as a warm water cloud or a very cold ice cloud), all investigated methods (BR, BTD and MTI) usually provide correct cloud phase identification.

7. MODIS Bands Ratio Cloud Phase Detection Algorithm – Collection 005

The MODIS algorithms are continuously being improved to provide more accurate retrievals of atmospheric data. Recently, a significant modification of the bands ratio part of the MODIS cloud phase detection algorithm has been developed and currently the MODIS imagery is being re-processed to provide a more accurate phase determination for future research. The modified set of thresholds plus the use of additional MODIS bands are a part of *Collection 005*, as described in *King et al.* [2005] and Table 4.

The results of the band ratio cloud phase detection with the *Collection 005* thresholds applied to the Katrina image are shown in Fig. 6. The band ratio detection with the thresholds for use over the land is still unable to properly identify the warmer part of the Katrina cloud as water (Fig. 6a). The situation is slightly improved when the thresholds designated for cloud over ocean (Table 4) are used (Fig. 6b). The full MODIS NIR cloud phase algorithm (MODIS cloud products MOD06 and MYD06) combines the MODIS cloud mask, with the BTD and the band ratio described above, leads to cloud phase identification shown in Fig. 6c. This ice/water distribution is in agreement with the expectations based on cloud top temperature, cloud particle size and with the MTI cloud phase detection results.

8. Summary and Conclusion

We have compared the band ratio (BR) and the brightness temperature difference (BTD) cloud phase retrieval procedures for the case of optically thick clouds and we

found that

i) The BTD cloud phase algorithm leads to results that we found to be in agreement with expectations based on the MODIS 11 μm cloud top brightness temperature (water for $T_{11} > 275$ K and ice for $T_{11} < 238$ K).

ii) The BR cloud phase detection (using thresholds from the MODIS *Collection 004*) was biased towards the ice phase. Often ice was identified when the 11 μm cloud top brightness temperature was above 275 K and when the BTD algorithm indicated water clouds. When the thresholds for clouds over land and sea were replaced by thresholds designated for clouds over snow and ice, the bias was shifted strongly in the opposite direction toward the water phase.

iii) The MTI (Multispectral Thermal Imager) NIR algorithm applied to the MODIS images provided cloud phase detection very similar to the BTD algorithm. The MTI results are also in agreement with expectations based on the cloud top brightness temperature and particle effective size.

iv) The complete MODIS cloud phase product (MOD06 and MYD06) that uses a combination of the MODIS cloud mask with the BTD and BR cloud detection method and the overriding cloud top temperature condition was found to be in agreement with expectations based on the cloud top radiative temperature and cloud particle size.

Pairs of VNIR multispectral bands in isolation (BR method) are not reliable means to determine thermodynamic phase of clouds in the terrestrial atmosphere (although the bands used in the MTI code seem to be more reliable than those used as a part of MODIS code). The NIR multispectral bands provide supporting evidence of cloud phase for opti-

cally thick clouds, but using TIR tests and temperature "sanity" checks are also required (as is done in producing the MODIS cloud phase products MOD06 and MYD06) to obtain a reliable determination of cloud phase. Although our examples seem to suggest that BTD alone might be good for cloud phase detection, there are situations (clouds above snow and ice surfaces, for example) where the BTD algorithm alone is problematic. Hence, in multispectral remote sensing it is advisable to take advantage of both shortwave and longwave bands to determine the cloud phase.

For future development of cloud phase detection algorithms for hyperspectral TIR instruments, an analogue of the MODIS algorithm based on bands centered around 11 and 8.55 μm will be a good starting point. For the NIR hyperspectral instruments it is possible to improve the current multispectral methods of the cloud phase detection. An attractive possibility seems to be the use of the ratio of the NIR hyperspectral bands around 1.5 and 1.4 μm or around 2.05 and 1.9 μm (Fig. 1).

Acknowledgment. The reported research was partially supported by Los Alamos National Laboratory's Directed Research and Development Project entitled "Resolving the Aerosol-Climate-Water Puzzle (20050014DR)" and by the "Mixed Phase Cloud" project supported by the University of California Institute of Geophysics and Planetary Physics.

References

Baum, B. A., P. F. Soulen, K. I. Strabala, M. D. King, S. A. Ackerman, W. P. Menzel, and P. Yang, Remote sensing of cloud properties using MODIS Airborne Simulator imagery during SUCCESS. II: Cloud thermodynamic phase, *J. Geophys. Res., 105,* 1781-11792, 2000.

Chylek, P., B. Henderson, and M. Mishchenko, Aerosol radiative forcing and the accuracy of satellite aerosol optical depth retrieval, *J. Geophys. Res., 108*, doi:10.1029/2003JD004044, 2003.

Chylek, P., and C. Borel, Mixed phase cloud water/ice structure from high spatial resolution satellite data, *Geophys. Res. Lett., 31,* doi:10.1029/2004GL020428, 2004.

Chylek, P., M. K. Dubey, U. Lohmann, V. Ramanathan, Y. Kaufman, G. Lesins, J. Hudson, G. Altmann, and S. Olsen, Aerosol indirect effect over the Indian Ocean, *Geophys. Res. Lett.,* in press, 2006.

Fu, Q., An accurate parameterization of the solar radiative properties of cirrus clouds for climate models, *J. Climate, 9,* 2058-2082, 1996.

Fu, Q., P. Yang, and W. Sun, An accurate parameterization of the infrared radiative properties of cirrus clouds for climate models, *J. Climate, 25,* 2223-2237, 1998.

Gosse, S., D. Labrie, and P. Chylek, Refractive index of ice in the 1.4 to 7.8 μm spectral range, *Appl. Opt., 34,* 6582-6586, 1995.

Hale, G. and M. Querry, Optical constants of water in the 200 nm to 200 μm wavelength region, *Appl. Opt., 12,* 555-563, 1973.

Kaufman, Y. J., D. Tanré, L. A. Remer, E. F. Vermote, A. Chu and B. N. Holben, Operational remote sensing of tropospheric aerosol over land from EOS moderate resolu-

tion imaging spectroradiometer, *J. Geophys. Res.*, *102*, 17051-17067, 1997.

Kaufman, Y. J., D. Tanré, and O. Boucher, A satellite view of aerosols in the climate system, *Nature, 419,* 215-223, 2002.

King, M. D., Y. J. Kaufman, W. P. Menzel, and D. Tanré, Remote sensing of cloud, aerosol, and water vapor properties from the Moderate Resolution Imaging Spectrometer (MODIS), *IEEE Trans. Geosci. Remote Sensing, 30,* 2-27, 1992.

King, M. D., S.-C. Tsay, S. Platnick, M. Wang, and K.-N. Liou, Cloud Retrieval Algorithms for MODIS: Optical Thickness, Effective Particle Radius, and Thermodynamic Phase, MODIS Algorithm Theoretical Basis, Document No. ATBD-MOD-05, MOD06-Cloud Product, modis-atmos.gsfc.nasa.gov/_docs/atbd_mod05.pdf, 1997.

King, M. D., S. Platnick, J. Riédi, MODIS Cloud Thermodynamic Phase Flowchart, modis-atmos.gsfc.nasa.gov/MOD06_L2/atbd.html, *Collection 004*, 2002.

King, M. D., W. P. Menzel, Y. J. Kaufman, D. Tanré, B. C. Gao, S. Platnick, S. A. Ackerman, L. A. Remer, R. Pincus, and P. A. Hubanks, Cloud and Aerosol Properties, Precipitable Water, and Profiles of Temperature and Humidity from MODIS, *IEEE Trans. Geosci. Remote Sens., 41,* 442-458, 2003.

King, M. D, S. Platnick, P. Yang, G. T. Arnold, M. A. Gray, J. C. Riédi, S. A. Ackerman, and K. N. Liou, Remote Sensing of Liquid Water and Ice Cloud Optical Thickness and Effective Radius in the Arctic: Application of Airborne Multispectral MAS Data, *J. Atmos. Ocean Technol., 21,* 857-875, 2004.

King, M., S. Platnick, J. Riédi, MODIS Cloud Thermodynamic Phase Flowchart, modis-atmos.gsfc.nasa.gov/MOD06_L2/atbd.html, *Collection 004*, 2005.

Kou, L., D. Labrie, and P. Chylek, Refractive index of water and ice in the 0.65 to 2.5 μm

spectral range, *Appl. Opt., 32,* 3531-3540, 1993.

Mishchenko, M. I., W. B. Rossow, A. Macke, and A. A. Lacis, Sensitivity of cirrus cloud albedo, bidirectional reflectance and optical thickness retrieval accuracy to ice particle shape, *J. Geophys. Res., 101,* 16973-16985, 1996.

Nakajima, T., and M. D. King, Determination of the optical thickness and effective particle radius of clouds from reflected solar radiation measurements. Part I: Theory, *J. Atmos. Sci*., *47*, 1878-1893, 1990.

Platnick, S., Vertical photon transport in cloud remote sensing problems, *J. Geophys. Res*., *105*, 22919-22935, 2000.

Platnick, S., M. D. King, S. A. Ackerman, W. P. Menzel, B. A. Baum, J. C. Riédi, and R. A. Frey, The MODIS cloud products: Algorithms and examples from Terra, *IEEE Trans. Geosci. Remote Sens*., *41*, 459-473, 2003.

Strabala, K. I., S. A. Ackerman, and W. P. Menzel, Cloud properties inferred from 8-12-μm data, *J. Appl. Meteor., 33,* 212-229, 1994.

Tanré, D., Y. Kaufman, M. Herman, and S. Mattoo, Remote sensing of aerosol properties over oceans using the MODIS/EOS spectral radiances, *J. Geophys. Res., 102,* 16971-16988, 1997.

Warren, S., Optical constants of ice from the ultraviolet to the microwave, *Appl. Opt., 23,* 1206-1225, 1984.

Yang, P., H. L. Wei, H. L. Huang, B. A. Baum, Y. X. Hu, G. W. Kattawar, M. I. Mishchenko, and Q. Fu., Scattering and absorption property database for nonspherical ice particles in the near- through far-infrared spectral region, *Appl. Opt., 44,* 5512-5523, 2005.

Table 1: Visible, near infrared and thermal infrared MODIS bands used in the thermodynamic cloud phase detection in this study.

MODIS Band	Pixel Resolution (m)	Band Center (nm)	Band Width (nm)
1	250	645	50
2	250	859	25
3	500	469	20
4	500	555	20
5	500	1245	20
6	500	1640	24
7	500	2130	50
29	1000	8550	300
31	1000	11030	500

Table 2: Thresholds used in our study for the MODIS band ratio (BR) (*Collection 004*) [*King et al.,* 2002; 2004], BTD (based on *Baum et al.,* [2000]) and MTI [*Chylek and Borel,* 2004] cloud phase detection algorithms. The values in between the ice and water thresholds are interpreted as either undetermined or mixed phase clouds. R stands for reflectivity, T for cloud top radiative temperature, and Rad for radiance; the subscripts refer to the central wavelength (in μm) of the MODIS bands used.

	Ice	Water
MODIS BR B7/B1	$R_{2.13}/R_{0.66} < 0.35$	$R_{2.13}/R_{0.66} > 0.65$
Over Ocean and Land		
MODIS BR B7/B1	$R_{2.13}/R_{0.66} < 0.15$	$R_{2.13}/R_{0.66} > 0.45$
Over Ice and Snow		
MODIS BTD B29, B31	$T_{8.55}-T_{11} > 0.5$ K	$T_{8.55}-T_{11} < -1.0$ K
MTI B2/B6	$Rad_{0.86}/Rad_{1.62} > 11$	$Rad_{0.86}/Rad_{1.62} < 8$

Table 3: The color code used in Figs. 4 to 6; r_{eff} stands for the effective radius of cloud particles and T_{11} for the cloud top brightness temperature in MODIS band 31 (at 11 μm).

Color code	Cloud Phase	Cloud Top T_{11}	Effective Radius
Red	Ice	$T_{11} < 238$ K	$r_{eff} > 30$ μm
Yellow	Mixed or Undetermined	238 K $< T_{11} <$ 275 K	15 μm $< r_{eff} <$ 30 μm
Green	Water	$T_{11} > 275$ K	$r_{eff} < 15$ μm
Blue	Not a Cloud	Not a Cloud	Not a Cloud
Magenta	Undetermined		
Black	No Data	No Data	No Data

Table 4: *Collection 005* Thresholds for separating water and ice used in the modified MODIS bands ratio cloud phase detection. See Table 1 for specification of the used MODIS bands 1, 5 and 7.

	Ice	Water
MODIS BR B7/B1 Over Land	$R_{2.13}/R_{0.66} < 0.25$	$R_{2.13}/R_{0.66} > 0.55$
MODIS BR B7/B5 Over Ocean and Coastal Regions	$R_{2.13}/R_{1.24} < 0.20$	$R_{2.13}/R_{1.24} > 0.45$

Figure Captions

Fig. 1: The imaginary parts of refractive indices of water and ice in the 1.2 to 2.4 μm spectral region.

Fig. 2: The imaginary parts of refractive indices of water and ice in the 0.4 to 20 μm spectral region.

Fig. 3: False color images (MODIS bands 1, 2 and 3) clearly depicting clouds against the sea and the land. The indicated regions I, II, III, IV and V are selected for comparison of cloud phase detection schemes.

Fig. 4: Region I of Katrina image (Fig. 3) showing (a) the primitive cloud mask, (b) detection results using the band ratio (BR) part of the MODIS cloud phase algorithm, (c) cloud phase detection results using the brightness temperature difference (BTD) part of the MODIS algorithm, (d) 11 μm cloud top brightness temperature (MODIS band 31), (e) cloud phase detection results using the MTI near infrared algorithm, and (f) the MODIS retrieval of cloud particle effective size. See Table 3 for the definition of colors used.

Fig. 5: Region II of the Katrina image (Fig. 3) showing (a) primitive cloud mask, (b) cloud phase detection results using the BR part of the MODIS cloud phase algorithm, (c) cloud phase detection results using the BTD part of MODIS cloud phase algorithm, (d) 11 μm cloud top brightness temperature (MODIS band 31), (e) cloud phase detection results using the MTI near infrared algorithm, and (f) the MODIS retrieval of cloud particle effective size. See Table 3 for the definition of colors used.

Fig. 6: Cloud phase detection results using the modified MODIS BR algorithm with thresholds (*Collection 005*) designated for clouds over land (a) and over oceans

and coastal regions (b). For comparison, the current MODIS cloud phase product (MOD06) that uses a combination of the BTD and BR cloud detection and a cloud top temperature "sanity" check is also shown (c).

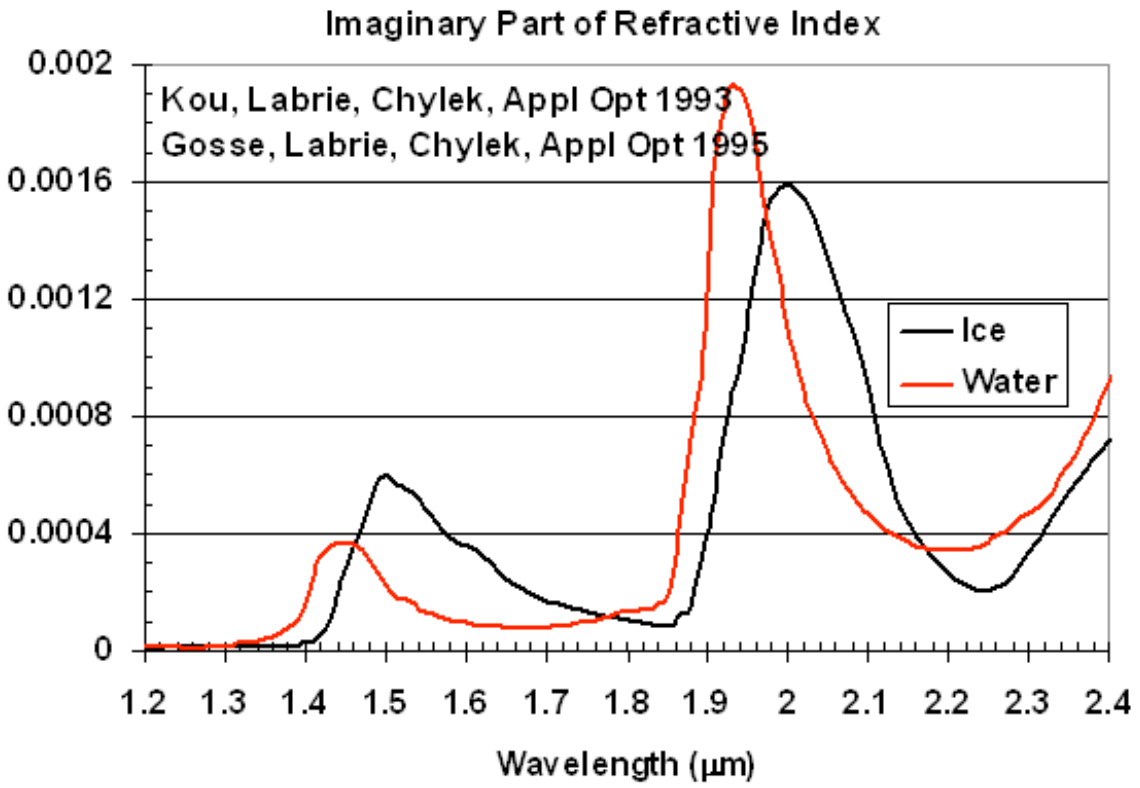

Fig. 1. The imaginary parts of refractive indices of water and ice in the 1.2 to 2.4 μm spectral region.

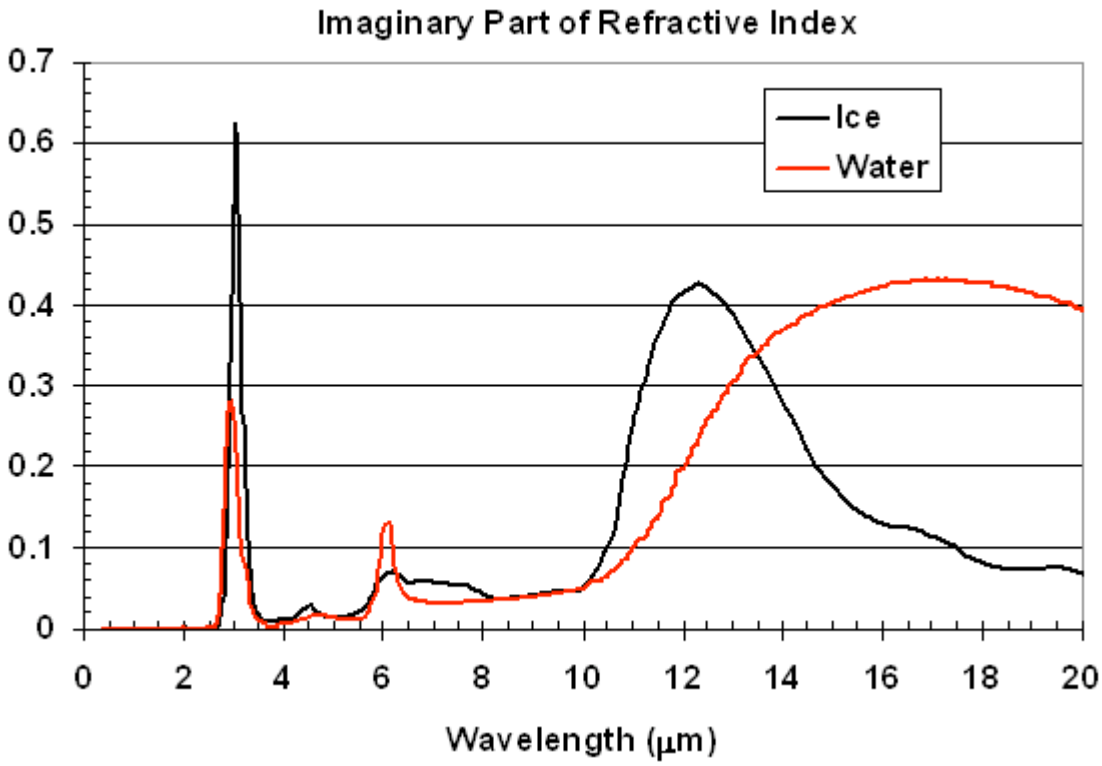

Fig. 2. The imaginary parts of refractive indices of water and ice in the 0.4 to 20 μm spectral region.

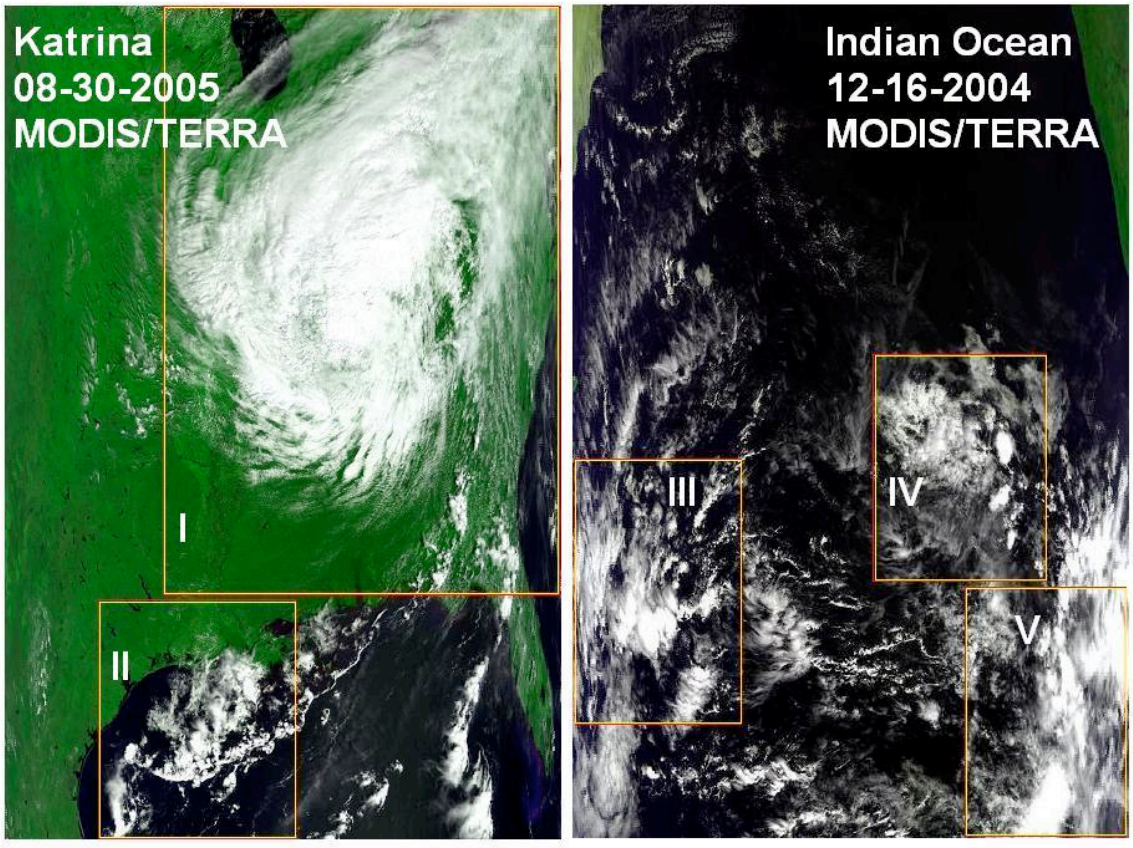

Fig. 3. False color images (MODIS bands 1, 2 and 3) clearly depicting clouds against the sea and the land. The indicated regions I, II, III, IV and V are selected for comparison of cloud phase detection schemes.

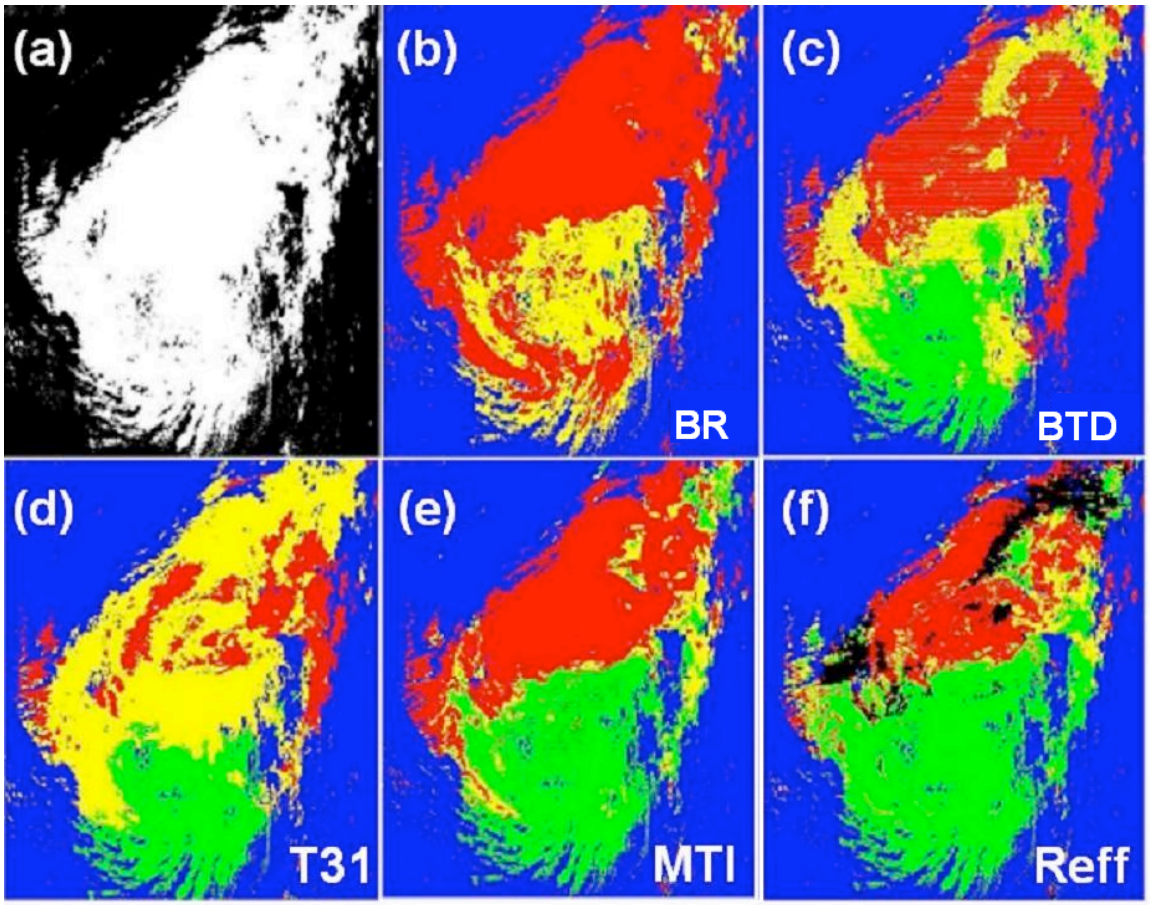

Fig. 4. Region I of Katrina image (Fig. 3) showing (a) the primitive cloud mask, (b) detection results using the band ratio (BR) part of the MODIS cloud phase algorithm, (c) cloud phase detection results using the brightness temperature difference (BTD) part of the MODIS algorithm, (d) 11 mm cloud top brightness temperature (MODIS band 31), (e) cloud phase detection results using the MTI near infrared algorithm, and (f) the MODIS retrieval of cloud particle effective size. See Table 3 for the definition of colors used.

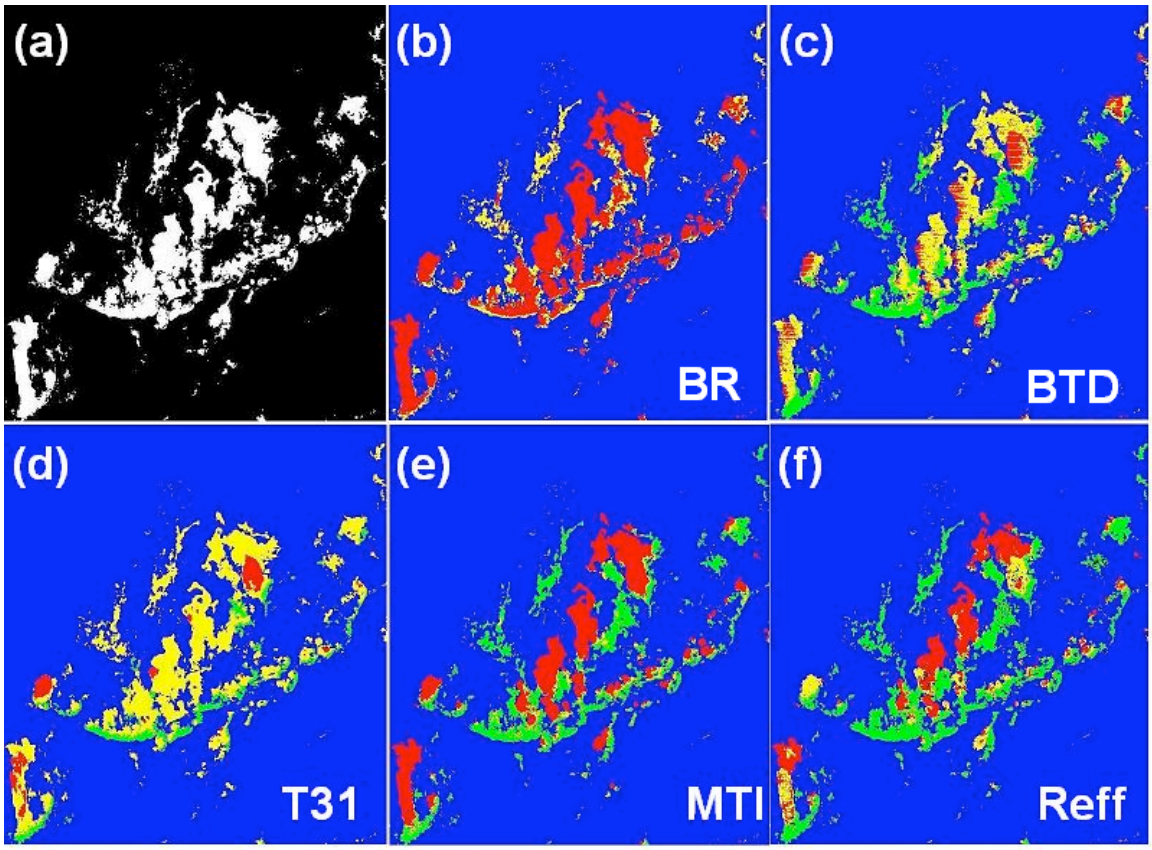

Fig. 5. Region II of the Katrina image (Fig. 3) showing (a) primitive cloud mask, (b) cloud phase detection results using the BR part of the MODIS cloud phase algorithm, (c) cloud phase detection results using the BTD part of MODIS cloud phase algorithm, (d) 11 mm cloud top brightness temperature (MODIS band 31), (e) cloud phase detection results using the MTI near infrared algorithm, and (f) the MODIS retrieval of cloud particle effective size. See Table 3 for the definition of colors used.

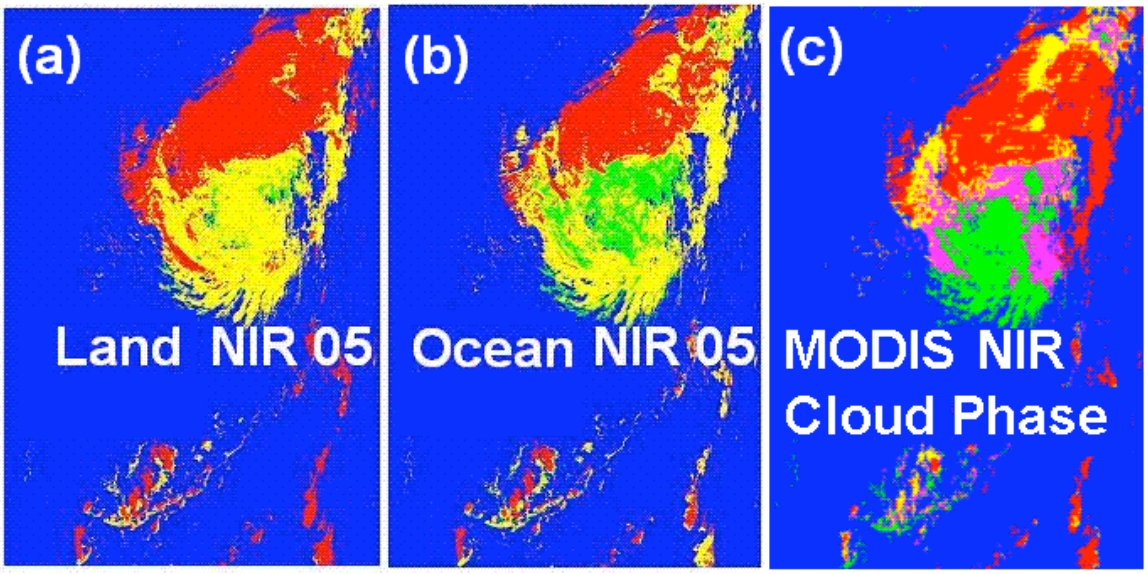

Fig. 6. Cloud phase detection results using the modified MODIS BR algorithm with thresholds (*Collection 005*) designated for clouds over land (a) and over oceans and coastal regions (b). For comparison, the current MODIS cloud phase product (MOD06) that uses a combination of the BTD and BR cloud detection and a cloud top temperature "sanity" check is also shown (c).